CHEMICAL AND MORPHOLOGICAL EVIDENCE FOR THE CONVERSION OF SMECTITE TO ILLITE

Atsuyuki Inoue,[1] Norihiko Kohyama,[2] Ryuji Kitagawa,[3] and Takashi Watanabe[4]

[1] Geological Institute, College of Arts & Sciences, Chiba University, Chiba 260, Japan

[2] National Institute of Industrial Health, The Ministry of Labor, Nagao, Tama-ku, Kawasaki 213, Japan

[3] Faculty of Science, Hiroshima University, Higashisendamachi, Naka-ku, Hiroshima 730, Japan

[4] Joetsu University of Education, Joetsu, Nigata 943, Japan

Abstract—The continuous conversion of smectite to illite in samples from the Shinzan hydrothermal alteration area of Japan has been examined by X-ray powder diffraction (XRD) and transmission (TEM) and analytical transmission electron microscopy (AEM). TEM shows that randomly interstratified illite/smectite (I/S) containing 100–50% expandable layers exhibits a flakey shape, whereas regularly and partially ordered interstratified I/S having 50–0% expandable layers exhibits a lath-like habit. An early-formed lath of regularly interstratified I/S is typically <35 Å in thickness and 300–500 Å in width; these dimensions gradually increase with decreasing percentage of expandable layers. XRD shows that the lath-shaped I/S has a 1*M* polytype mica structure. AEM shows that the interlayer K content of flakey I/S increases monotonously with decreasing percentage of expandable layers in the range 100–50% expandable layers, whereas the interlayer K content of lath-shaped I/S increases along a different trend from that for the flakey I/S in the range 50–0% expandable layers. These observations suggest that randomly interstratified I/S is fundamentally smectite that is undergoing K-fixation and dissolution and that regularly and partially ordered interstratified I/S are immature illite which is still growing. Consequently, they suggest a mechanism for the hydrothermal smectite-to-illite conversion that is based on the K-fixation in and dissolution of smectite and the precipitation and growth of thin illite particles. Furthermore, these data suggest that the kinetics of smectite dissolution and illite growth are the most important factors controlling the smectite-to-illite conversion.

Key Words—Diagenesis, Expandable layers, Illite, K-fixation, Smectite, X-ray powder diffraction.

要旨－秋田県真山熱水変質帯におけるスメクタイト－イライト変換系列を粉末X線回折・透過型および分析電子顕微鏡を用いて研究し、変換反応機構を明らかにした。イライト／スメクタイト(I/S) 混合層鉱物の結晶形態は、膨潤層100-50%の範囲では薄片状、50-0%の範囲では短柵状を示す。規則型 I/S の短柵は、厚さ35Å以下、幅 300-500Åのサイズを特徴としており、これらのサイズは、膨潤層の減少につれて次第に大きくなる。また、短柵状 I/Sは、1Mポリタイプの構造をもっている。非交換性K含有量は膨潤層100-50%の範囲の薄片状I/S では膨潤層の減少につれて単調に増加するが、50-0%の短柵状形態のものでは、別の経路を辿って増加する。これらの観察はランダム型 I/S混合層鉱物は基本的にはKの固定と溶解を起こしつつあるスメクタイトであり、規則型 I/S混合層鉱物は、現在成長しつつある未成熟のイライトとみなせることを示唆しており、これらに基づいた１つのスメクタイト－イライト変換反応機構が提出される。更に、これらのデータは、スメクタイト－イライト変換反応をコントロールする要因として、スメクタイトの溶解とイライトの成長のカイネティックスが重要であることを示唆している。

INTRODUCTION

Numerous clay mineralogical studies of shale, sandstone, and bentonite have shown that the conversion of smectite to illite through interstratified illite/smectite (I/S) is of great importance as a sensitive indicator or a geothermometer in estimating the degree of diagenesis of sediments (Dunoyer de Segonzac, 1970; Weaver and Beck, 1971; Foscolos and Kodama, 1974; Hower *et al.,* 1976; Hoffman and Hower, 1979; Hower,

1981). Such a conversion series has application in understanding the alteration processes in active and fossil geothermal fields (Steiner, 1968; Muffler and White, 1969; Browne and Ellis, 1970; Eslinger and Savin, 1973; Inoue and Utada, 1983; Horton, 1985; Jennings and Thompson, 1986). Previous mineralogical data have suggested a conversion mechanism in which illite forms from smectite by means of cation substitution in smectite layers (Hower *et al.,* 1976; Boles and Franks, 1979). Recently Pollastro (1985) supported this solid-state
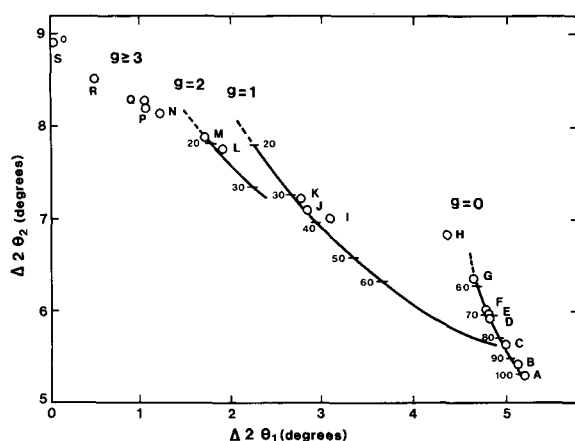
Figure 1.   Diagram showing $\Delta 2\theta_1$ vs. $\Delta 2\theta_2$ for illite/smectites used in this study.

Table 1.   Illite/smectite interstratified minerals from the Shinzan hydrothermal alteration area in Japan.

Sample	Drillhole	Depth (m)	Mineralogy[1]
A	WS-2	183.50	100% smectite
B	WS-1	336.75	95 ± 5% I/S (g = 0)
C	WS-4	329.50	85 ± 5% I/S (g = 0)
D	WS-4	383.00	73 ± 5% I/S (g = 0)
E	WS-2	377.80	70 ± 5% I/S (g = 0)
F	WS-2	407.35	68 ± 5% I/S (g = 0)
G	WS-2	383.80	55 ± 5% I/S (g = 0)
H	WS-4	392.80	50 ± 10% I/S (g = 0)
I	WS-2	423.20	40 ± 5% I/S (g = 1)
J	WS-10	199.90	35 ± 5% I/S (g = 1)
K	WS-4	440.60	30 ± 5% I/S (g = 1)
L	WS-2	622.25	23 ± 5% I/S (g = 2)
M	WS-5	240.10	20 ± 5% I/S (g = 2)
N	WS-7	123.60	15 ± 5% I/S (g ≥ 3)
P	WS-7	115.45	15 ± 5% I/S (g ≥ 3)
Q	WS-5	185.90	12.5 ± 2.5% I/S (g ≥ 3)
R	WS-7	197.00	5 ± 5% I/S (g ≥ 3)
S	WS-8	452.80	0% illite

[1] Mineralogy by X-ray powder diffraction of ethylene glycol-solvated samples using the method of Watanabe (1981). g stands for the Reichweite value.

transformation process for the smectite-to-illite conversion which requires partial dissolution of smectite layers in more expandable I/S substrates and reprecipitation of dissolved materials on less expandable I/S clays.

On the other hand, Nadeau *et al.* (1984b, 1985) advocated an alternative neoformation process for the smectite-to-illite conversion on the basis of particle-thickness measurements of highly dispersed I/S clays by transmission electron microscopy. They demonstrated that randomly interstratified I/S can be formed from physically mixed suspensions of elementary smectite (10-Å thick) particles and "illite" (20-Å thick) particles; the "illite" particle corresponds to a rectorite-type interstratified mineral (Nadeau *et al.,* 1984a). The X-ray powder diffraction (XRD) patterns of well-known IS-, IIS-, and IIIS-type ordered minerals as described by Reynolds and Hower (1970) were interpreted as interparticle diffraction effects wherein water and organic molecules are adsorbed on the smectite-like interfaces within aggregates of thin "illite" crystals (Nadeau *et al.,* 1985). Furthermore, they applied the neoformation process, based on this concept of interparticle diffraction, to the conversion of smectite to illite in bentonites and sandstones. Their idea undoubtedly sheds new light on the concept of interstratification; however, several issues regarding their interpretation are still unresolved, particularly the chemical nature of the neoformed clay particles. In addition, although the samples used in their studies were from various geological settings, the conversion of smectite to illite was considered to occur by a common mechanism.

In the present investigation, transmission electron microscopy (TEM) and analytical electron microscopy (AEM) techniques in addition to ordinary X-ray powder diffraction (XRD) techniques were used to examine the morphological and chemical changes in a hydro-

thermal smectite-to-illite conversion series from the Shinzan area of Japan.

SAMPLES AND EXPERIMENTAL METHODS

Interstratified I/S minerals from the Shinzan area were probably formed by the hydrothermal alteration of silicic volcanic glass during Kuroko ore mineralization or during later vein-type ore mineralization in the Miocene Period. As described by Inoue *et al.* (1978) and Inoue and Utada (1983), a complete smectite illitization series is present from the center of the hydrothermally altered mass to the margin in the Shinzan area. In the present study, 18 samples of the I/S clays were used, as listed in Table 1.

The <1-μm fractions of untreated clay samples were isolated by centrifugation. The suspensions were smeared on glass slides, dried at room temperature, solvated with ethylene glycol (EG) vapor, and examined by XRD on a Rigaku RAD I-B diffractometer using monochromatized CuKα radiation, a 0.5° divergence silt, and a 0.6-mm receiving slit. The percentage of expandable layers and ordering type (Reichweite) of the I/S samples were determined using the $\Delta 2\theta_1 - \Delta 2\theta_2$ diagram of Watanabe (1981) (see Inoue and Utada, 1983). The definition of Reichweite (g) values used in this paper follows that of Jagodzinski (1949). The accuracy of the determination of the percentage of expandable layers was ±5% for most I/S samples, because the d-values of EG-clay complexes are sensitive to the nature of component layers and EG-vapor pressure (Środoń, 1980). The accuracy for sample H, may be as low as ±10% because of the interference of discrete illite.
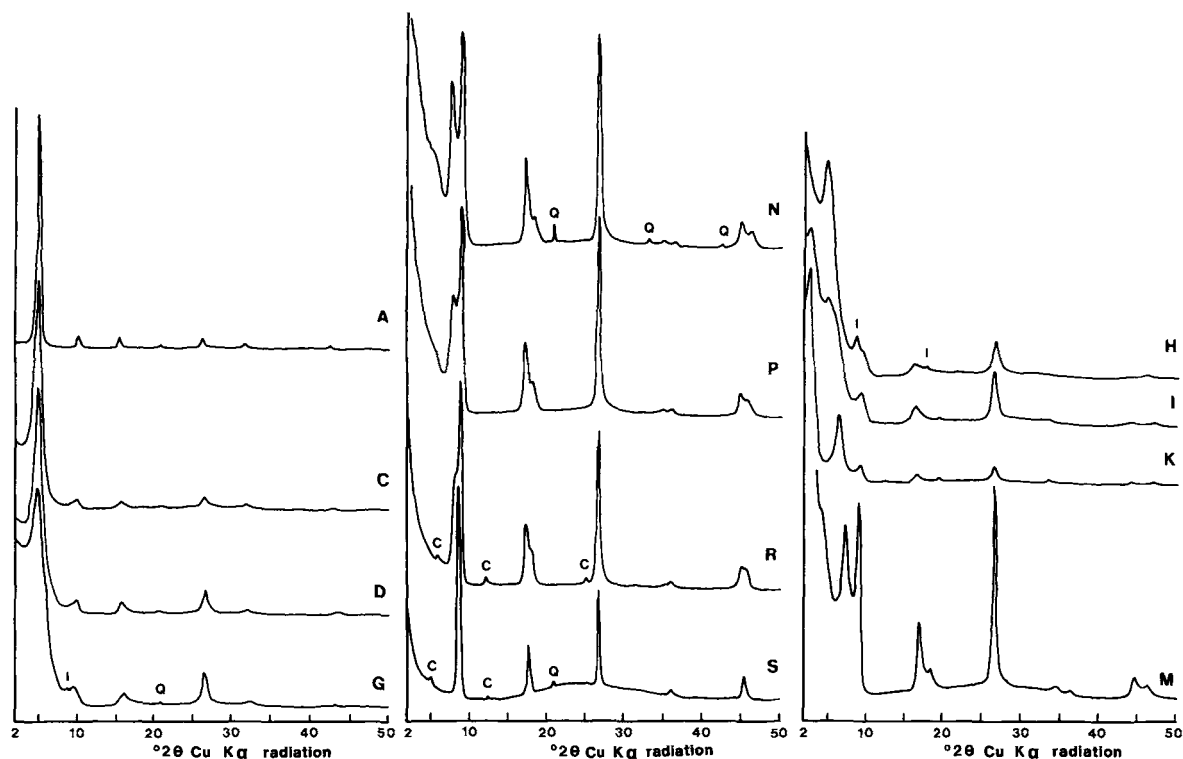
Figure 2. X-ray powder diffraction patterns of illite/smectites from samples A, C, D, G, H, I, K, M, N, P, R, and S after solvation with ethylene glycol. I = illite, Q = quartz, C = chlorite.

Chemical analysis was carried out with a Hitachi H-500 transmission electron microscope equipped with a Kevex 5000 solid-state detector for energy-dispersive X-ray analysis and a microcomputer for quantitative data processing. The accelerating voltage and beam current were 100 kV and about 240 pA, respectively; the relevant count time was arbitrarily adopted to minimize the beam damage of crystals of various thicknesses. Analyses were made only for Mg, Al, Si, K, Ca, and Fe(total); Na was neglected in this investigation. The measured X-ray intensity of each element was first corrected by subtracting the background intensity which was measured at two energy positions devoid of interference and then corrected using k-values obtained from kaolinite, muscovite, celadonite, and chlorite standard specimens. A linear relationship between the intensity of characteristic X-ray of each element and the total intensity can be established on a specimen thin enough for the conventional 100-kV electron microscopy. In such a thin area X-ray absorption and fluorescence can be neglected (Cliff and Lorimer, 1975). If the crystal analyzed was very thin (i.e., a few unit cells thick), the electron beam penetrated the crystal and the analysis was impossible. Thus, particles at least a few hundreds Ångstrom units thick were used to obtain useful X-ray signal/noise ratios.

For TEM examination, duplicates of specimens used for the AEM examination were prepared by spreading the sample on Ni TEM grids and shadowing it with Pt-Pd at an angle for which the ratio of the particle thickness to shadow length is 0.5. Shadow lengths of 20–75 particles and particle dimensions of 70–80 particles per sample were measured from micrographs. The accuracy of particle-thickness and particle-dimension determinations was ±6 Å and ±10 Å, respectively.

EXPERIMENTAL RESULTS

Interstratification by XRD

The $\Delta 2\theta_1$ vs. $\Delta 2\theta_2$ plots for the I/S clays examined are given in Figure 1; XRD patterns of the samples after EG-solvation are illustrated in Figure 2. As shown in Figures 1 and 2, sample A is pure smectite, having 100% expandable layers; samples B–G and probably H are randomly interstratified (g = 0) I/S. Although sample H plots in the intermediate field between g = 0 and g = 1 curves, the sample is contaminated by a small amount of discrete illite as shown in Figure 2. Thus, the accuracy of the $\Delta 2\theta_1$ and $\Delta 2\theta_2$ values is somewhat less. Samples I–K are regularly interstratified (g = 1) I/S; for samples L and M, g = 2, for samples N–R, g ≥ 3. Sample S is pure illite, having no expandable layer component.
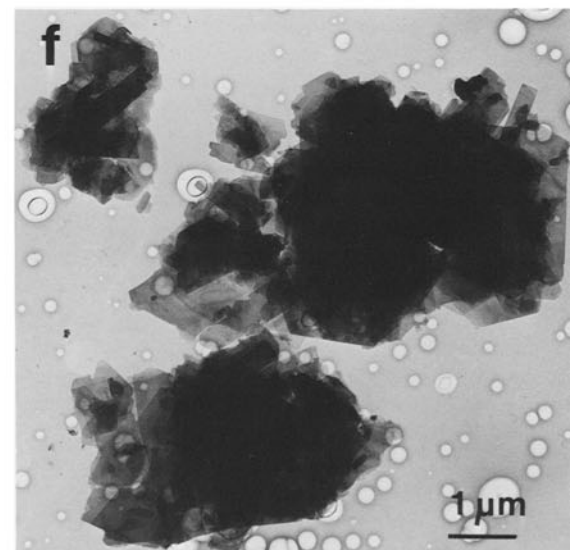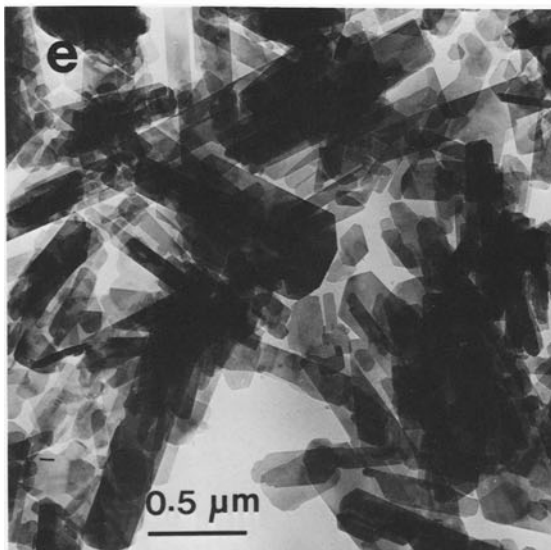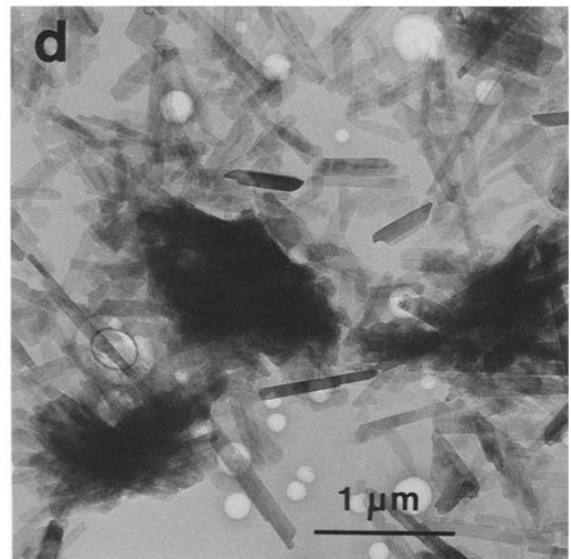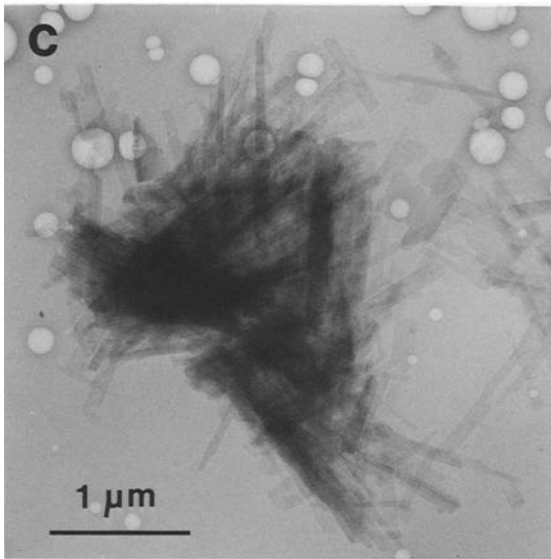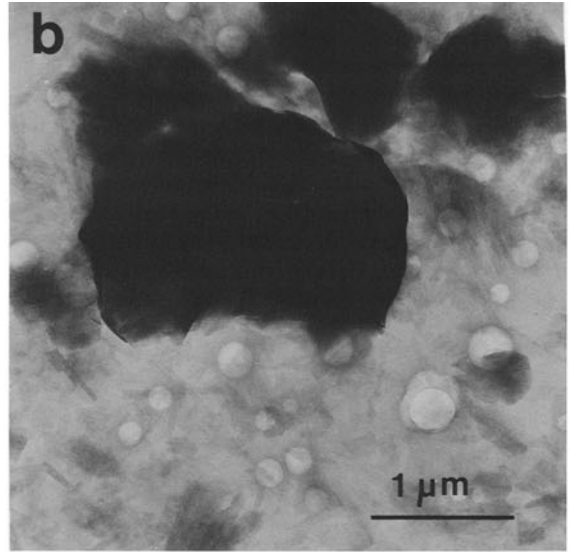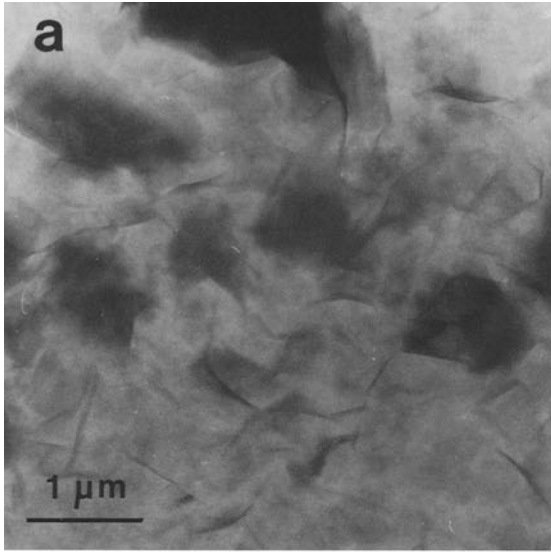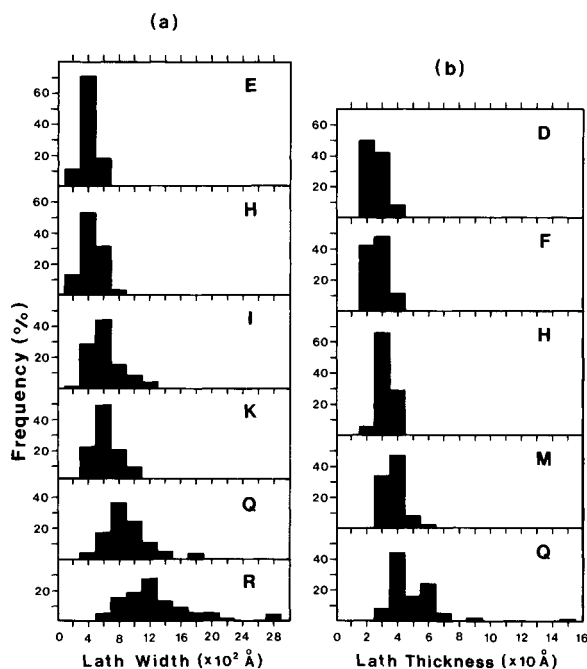
Figure 4. Histograms of lath-width distribution (a) and lath-thickness distribution (b) in illite/smectites from samples E, H, I, K, Q, and R for width and from samples D, F, H, M, and Q for thickness.

Morphology by TEM

TEM examination of the I/S series showed the following characteristic morphological changes with varying percentage of expandable layers. A particle of pure smectite is flake-like or moss-like and exhibits curling on its edges (Figure 3a). Anhedral flakes are dominant, but a euhedral hexagonal habit has been noted for some particles in the pure smectite sample. At 80–70% expandable layers, very thin lath-shaped particles coexist with dominant flake-like particles (Figure 3b). In these samples, some of the particles which appear to be flakes were found under high magnification to be dense aggregates of very thin laths. The flakey habit gradually disappeared with decreasing percentage of expandable layers. At <50% expandable layers, the particles were chiefly subhedral thin laths; no flakes were noted (Figures 3c and 3d). The laths were elongated along a, and the intensities of the 02, 11, and 1$\bar{1}$ reflections were consistently characteristic of the 1M polytype, according to Güven (1974). In addition, the laths were aggregated in a rather regular manner because the diffraction did not show the ring pattern typical of a perfect
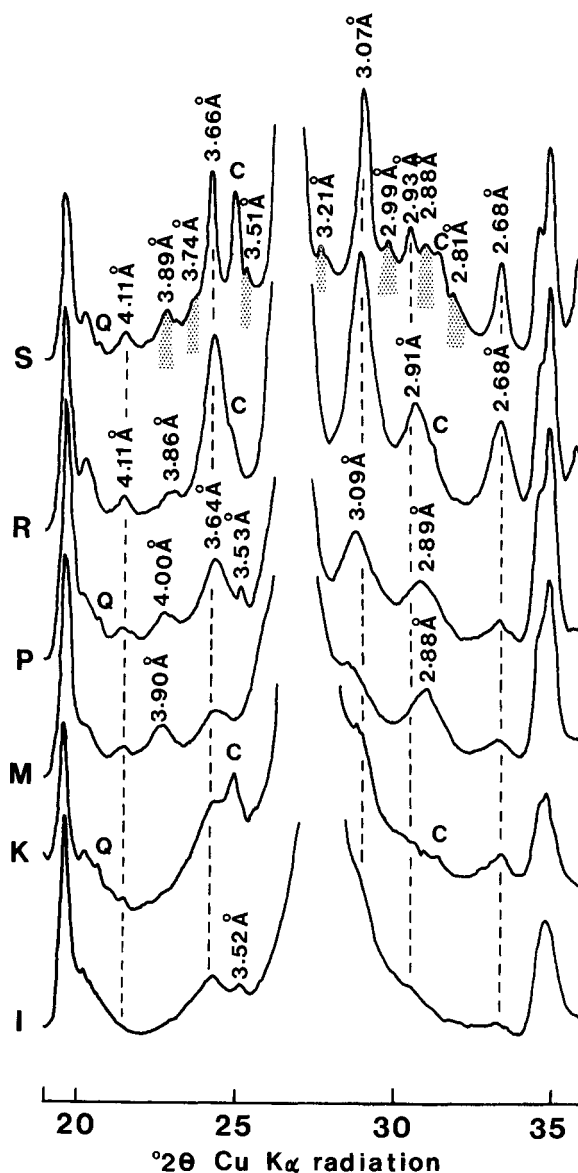

Figure 5. X-ray powder diffraction patterns of illite/smectites from samples I, K, M, P, R, and S measured in random preparations. Dashed lines indicate the positions of hkl reflections of 1M polytype; shadowed peaks represent hkl reflections of 2M_1 polytype. Q = quartz, C = chlorite.

turbostratic structure, but instead showed discrete hk spots with rings. Such a regular arrangement of laths has often been observed for illitic clays (Güven et al., 1980; Środoń and Eberl, 1984). Impure, discrete illite laths associated with the samples were easily distin-

←

Figure 3. Transmission electron micrographs of illite/smectites from (a) sample A, (b) sample D, (c) sample J, (d) sample L, (e) sample R, and (f) sample S.

Table 2. Structural formulae (/$O_{10}(OH)_2$) of illite/smectites having different morphologies, based on the analytical transmission electron microscopy analyses.

Sample	A	B	C	D	D	F	F	G	G	G	H	I
Morphology	flake	flake	flake	flake	lath	flake	lath	flake	lath	flake and lath stacked	lath	lath
Analyzed particle	4	5	1	12	2	5	4	2	14	4	6	18
Si	3.84(6)	3.81(3)	3.77	3.65(7)	3.70(5)	3.58(8)	3.57(14)	3.51(4)	3.52(7)	3.51(2)	3.59(8)	3.47(8)
Al	1.84(7)	1.59(3)	1.94	1.90(9)	1.85(13)	2.10(10)	2.11(6)	2.12(6)	2.15(9)	2.14(5)	1.96(5)	2.28(11)
Fe	0.08(1)	0.22(2)	0.13	0.14(2)	0.12(1)	0.13(2)	0.13(1)	0.13(1)	0.13(2)	0.13(1)	0.17(2)	0.10(2)
Mg	0.31(11)	0.54(6)	0.27	0.43(6)	0.43(9)	0.32(11)	0.32(15)	0.33(4)	0.32(8)	0.33(8)	0.42(8)	0.27(9)
Ca	0.08(3)	0.09(1)	0.04	0.08(2)	0.08(2)	0.04(3)	0.04(4)	0.07(1)	0.07(1)	0.07(1)	0.05(1)	0.05(1)
K	0.05(3)	0.08(1)	0.11	0.25(6)	0.26(2)	0.27(7)	0.29(9)	0.41(2)	0.29(7)	0.36(6)	0.31(9)	0.34(7)

Sample	J	J	K	K	L	M	M	Q	R	R	S	S
Morphology	lath	flake	lath	flake	lath	lath	flake	lath	lath	hexagonal	lath	hexagonal
Analyzed particle	5	5	7	3	16	5	5	13	21	3	3	9
Si	3.47(9)	3.41(8)	3.42(7)	3.44(11)	3.28(8)	3.25(10)	3.28(8)	3.22(6)	3.22(8)	3.37(14)	3.08(6)	3.13(9)
Al	2.21(8)	2.25(5)	2.28(7)	2.25(6)	2.47(10)	2.57(12)	2.49(13)	2.49(11)	2.51(12)	2.32(16)	2.73(11)	2.65(8)
Fe	0.11(1)	0.11(3)	0.07(1)	0.07(1)	0.08(2)	0.06(3)	0.07(2)	0.10(2)	0.07(2)	0.06(1)	0.04(1)	0.05(1)
Mg	0.29(10)	0.31(10)	0.37(6)	0.37(14)	0.25(8)	0.20(7)	0.20(9)	0.24(12)	0.24(15)	0.24(8)	0.19(5)	0.23(11)
Ca	0.08(1)	0.08(3)	0.05(2)	0.05(2)	0.06(2)	0.04(2)	0.05(1)	0.06(2)	0.06(3)	0.07(7)	0.08(1)	0.07(2)
K	0.43(10)	0.48(7)	0.44(15)	0.43(7)	0.59(9)	0.61(5)	0.71(2)	0.73(6)	0.76(6)	0.73(8)	0.80(1)	0.78(8)

The numerical figures in the parentheses indicate the standard deviations.

guished from I/S laths because of the greater thickness and thereby a high contrast image for the former. At <10% expandable layers, tiny hexagonal crystals (0.1–0.2 µm in size) together with dominant, euhedral lath-like crystals were common (Figure 3e). In pure illite, clearly hexagonal plate habits coexisted with rigid laths (Figure 3f).

The micrographs discussed above suggest that the lath-shaped crystals increase in thickness and width with decreasing percentage of expandable layers. The lath-width distribution (Figure 4a) shows that at 70% expandable layers (E) the laths are about 300–500 Å in width, in terms of the peak of distribution, and at 40% expandable layers (I) they are about 500–700 Å wide. Furthermore, at 5% expandable layers (R) the lath width is about 1100–1300 Å, with some laths of >2000 Å width also being present. The lath-thickness distribution (Figure 4b) shows that at 73% expandable layers (D) the lath thickness is mostly less than 35 Å, and confirms the morphological observation that the lath thickness also gradually increases with decreasing percentage of expandable layers. The particle-thickness distribution found here seems to be consistent with the observations of Nadeau et al. (1985).

Polytype by XRD

Figure 5 shows the hkl reflections in the range 19°–36°2θ of I/S clays having <50% expandable layers. Similar to pure smectite, I/S clays having >50% expandable layers exhibited turbostratic structure: only 02,11 and 20,13 prismatic reflections were observed in the same range of 2θ degrees. The I/S clay having 40% expandable layers (I) exhibited a few hkl reflections which could be indexed as from a 1M polytype of mica. These reflections sharpened with decreasing percentage of expandable layers. Samples M, P, and R exhibited another reflection at 3.86–4.00 Å which could not be indexed by the 1M polytype. The 11\overline{3} peak of 1M polytype tended to shift to higher angles. In the pure illite (S) several hkl reflections indexed by 2M₁ polytype were found in addition to the principal 1M polytype reflections. Taking into account the previous TEM observations, illite having a hexagonal habit probably has 2M₁ symmetry. XRD indicated that I/S clays exhibiting lath-like habit have a 1M mica polytype structure even if their percentage of expandable layers is large.

Chemical analyses by AEM

The empirical formulae of I/S clays calculated from AEM analyses on the basis of $O_{10}(OH)_2$ are listed in Table 2. These data were averaged from the analyses of 1–21 particles/sample. Generally speaking, the present AEM data are consonant with the "wet" chemical analyses reported by Inoue et al. (1978), except that the Si content is smaller and the Al, K, and Ca contents are somewhat larger in the AEM analyses.

The relationship between the percentage of expandable layers and the K content is shown in Figure 6, wherein all the K in the I/S clays has been assumed to be present as non-exchangeable interlayer cations. From these data, the K content of I/S having flakey habit and 100–50% expandable layers appears to increase monotonously with decreasing percentage of expandable layers, whereas the K content of I/S having a lath-like habit does not increase as much in the range 70–40% expandable layers and varies along a different trend from that of the flakey I/S. The increase in K content of I/S having a lath-like habit becomes significant in the range 40–20% expandable layers; in I/S having <20% expandable layers the increase in K is less steep and reaches a value of about 0.75–0.8 $K/O_{10}(OH)_2$. The relationship between the percentage of expandable layers and the total layer charges of I/S clays calculated from the data in Table 2 is similar to that found for the percentage of expandable layers and the K content.

Inoue and Utada (1983) demonstrated that the relationship between the percentage of expandable layers and K content can be expressed by a linear equation, percentage of expandable layers = -137 K $+ 103$, on the basis of wet chemical analyses of I/S samples, including the present samples. The data, however, correspond to the average of the chemical composition of morphologically different particles. In fact, the increase in K with decreasing percentage of expandable layers progresses along different paths between flake- and lath-like habit I/S clays as shown in Figure 6. On the other hand, Środoń and Eberl (1984) and Środoń et al. (1986) indicated from detailed statistical analyses of the percentage of expandable layers and the K contents of many different series of I/S, including the data of Inoue and Utada (1983), that the relationship is approximated by two curves of different slopes, percentage of expandable layers = -181.5 K $+ 102.3$ and = -99.21 K $+ 74.75$. The curves intersect at about 0.3 K and 46% expandable layers. The significance of the intersection reported by Środoń et al. (1986), however, is questionable considering the present study because I/S clays having lath-like habits begin to appear at 80–70% expandable layers, and the K contents are relatively constant in the range 70–40% expandable layers, as shown in Figure 6.

DISCUSSION

The present results regarding particle-thickness distribution seem to support the theory of interparticle diffraction by Nadeau et al. (1984a, 1984b, 1985). Nevertheless, applying their neoformation model based on the interparticle diffraction theory to the present smectite-to-illite conversion, several modifications for their model may be suggested.

For random I/S clays having 100–50% expandable layers (as noted above), Nadeau et al. (1984a) dem-
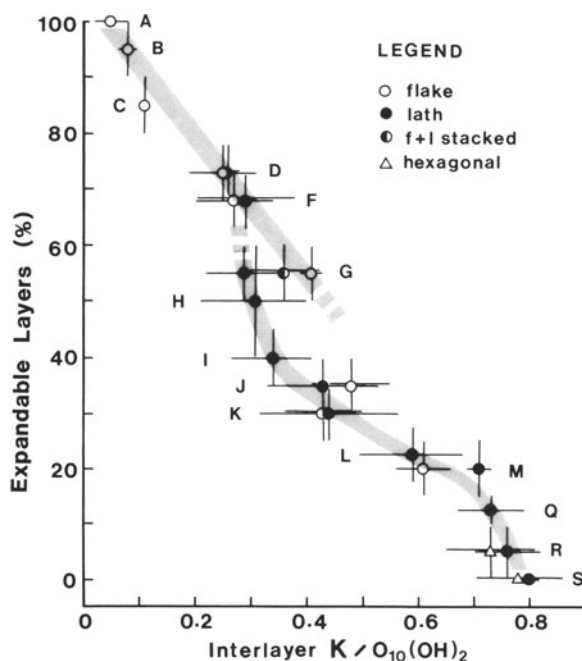

Figure 6. Relationship of percentage of expandable layers and fixed interlayer $K/O_{10}(OH)_2$ for illite/smectites. Symbols indicate morphology of each particle.

onstrated that the XRD patterns of mixed suspensions of 100% smectite and 50% regular I/S in various proportions show a strong resemblance to those of randomly interstratified I/S clays. They also predicted that the K contents in I/S clays will be proportional to the number of "illite" layers having a rectorite structure. In terms of the former proposal, unpublished data from this laboratory on the half-height width of the $(003)_{10}/(005)_{17}$ XRD peak after EG-solvation for mixtures of 100% smectite and 50% rectorite of various proportions indicated that the half-height width of mixtures tended to be greater than those of each end-member clay, showing a maximum at 1:1 mixture. The half-height width of the present I/S series after Sr-saturation and EG-solvation, however, showed a nearly monotonous decrease from 100 to 50% expandable layers. In terms of the second proposal by Nadeau et al. (1984a), Figure 6 shows that in samples D and F the K contents are almost the same for both the flake-like and lath-like habits. In sample G, however, having fewer expandable layers than samples D and F, the K contents of the lath-like and flake-like habits are clearly distinct: 0.3 for the laths and 0.4 for the flakes. In addition, the K contents of particles mixed with the flakes and the laths plot in the intermediate position between the respective values. These observations are contrary to the prediction of Nadeau et al. (1984a) and suggest that the randomly interstratified I/S clays are not physical mixtures of smectite and regular I/S, but that the randomly interstratified I/S clays having flake-like habits
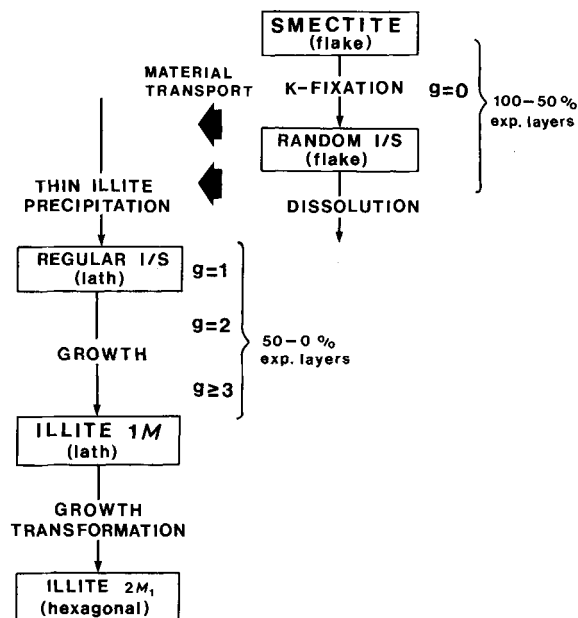
Figure 7. Possible mechanism for the continuous conversion of smectite to illite in the Shinzan hydrothermal alteration area.
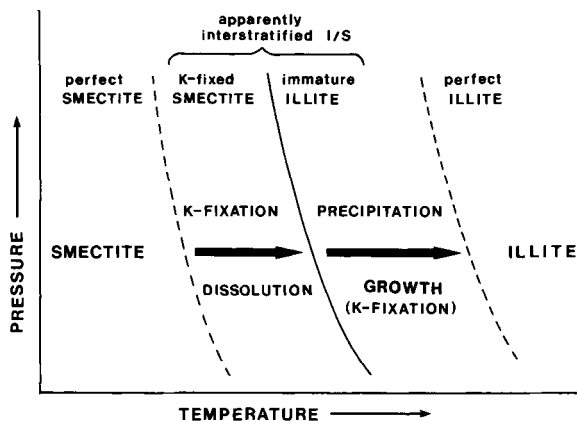

Figure 8. Schematic diagram showing the conversion of smectite to illite in nature. Slopes of the solid and dashed curves that represent the boundary between smectite and illite were assumed on the basis of occurrence of illite/smectite in many drillholes previously reported.

are structurally, morphologically, and chemically distinguished from the regularly interstratified I/S clays having lath-like habits. Consequently, the randomly interstratified I/S clays are fundamentally smectite that has adsorbed K in the interlayer spaces.

For less expandable I/S clays, if the increase in K content with decreasing percentage of expandable layers is attributed only to simple stacking of elementary "illite" particles (20-Å thick) of the model of Nadeau *et al.* (1984a), the K content will increase to a maximum of about 0.5 $K/O_{10}(OH)_2$ in pure illite. Accordingly, the fact that pure illite has 0.75–0.8 $K/O_{10}(OH)_2$ implies that K ions exist to some extent on the smectite-like interfaces between simply stacked elementary "illite" layers, as was diagrammatically represented in Figure 9 of Nadeau *et al.* (1984b). In other words, the smectite-like interfaces are developing into true illite layers with apparently decreasing percentage of expandable layers.

Finally, a possible mechanism for the present conversion series of smectite to illite is shown schematically in Figure 7. The I/S clays from the Shinzan hydrothermal alteration area were considered to be converted from early-formed smectite in turn according to the prevailing gradients of temperature and chemicals (Inoue and Utada, 1983). Therefore, the present process of smectite-to-illite conversion is very similar to those taking place in bentonites during diagenesis. In the conversion of smectite to illite as shown in Figure 7, interlayer K first increases in the flakey smectite by cation exchange and cation fixation, re-

sulting in the formation of randomly interstratified I/S clays having 100–50% expandable layers. At this stage, both the octahedral and tetrahedral layer charges have increased only slightly and the total layer charges of random I/S clays have reached a value of no more than about 0.5. Such randomly interstratified I/S clays having flake-like habit are structurally and morphologically unstable if the K contents in random I/S exceed about 0.4 or if the percentage of expandable layers <50%, resulting in the I/S clays dissolving and subsequently precipitating as "illite." Although the unstable flakey I/S clays dissolve, clays having lath-like habits begin to precipitate and are associated with flakey randomly interstratified I/S clays having 80–70% expandable layers. The initial precipitates having lath-like habits may be elementary "illite" layers (20-Å thick) having insufficient K on the two outer-interfaces of 2:1 silicate layers and a regularly interstratified structure of g = 1, which is the same as the model of Nadeau *et al.* (1985). The elementary "illite" particle has a 1*M* polytype structure and therefore can be regarded as an immature or embryonic illite. Furthermore, the laths thicken by growing. In the growth stage the lath-like illite exhibits various kinds of interstratifications, such as g = 2 and g ≥ 3, according to the layer-thickness or the heterogeneity in the tetrahedral layer charge. If the laths grow larger, they may break along certain crystallographic directions to create hexagonal plates and finally transform to a 2*M*₁ polytype mica.

The smectite-to-illite conversion mentioned above is neither a continuous transformation process by solid-state reaction nor a neoformation process associated with stepwise dissolution-precipitation previously proposed. The present conversion can be considered to be a complex neoformation process consisting of two elementary transformation reactions and a dissolution-

precipitation reaction in the intermediate stage. The random interstratification that occurred in the range 100–50% expandable layers can be principally responsible for the K-fixation of initial smectite; this stage can be represented by a transformation process. The regular and partially ordered interstratifications in the range 50–0% expandable layers result from the layer-thickness of immature illite growth; this stage can be also a transformation process. During these two transformation reactions, unstable smectite dissolves and reprecipitates as elementary illite particles.

In a stricter sense, however, the above interpretation suggests that the interstratification generated in the smectite-to-illite conversion is a secondary phenomenon associated with the chemical conversion of smectite to illite in nature (Figure 8). Specifically, the conversion of smectite to illite requires material transport; this reaction might be formally expressed as smectite + Al + K = illite + Si. The present experimental results suggest that the conversion is due to the dissolution of smectite and the precipitation and growth of illite. In general, the dissolution, precipitation, and growth of minerals occur over a finite time period and are strongly sensitive to ambient conditions. If the conversion of smectite to illite is a simple solid-solid transition, the conversion can be expressed by a univariant curve in a P-T region, as represented by the solid curve in Figure 8. Because, however, the conversion of smectite to illite is a complex chemical reaction of dissolution, precipitation, and growth with material transport, the conversion apparently occurs in a broad P-T region, as represented by the area between the two dashed curves in Figure 8. The interstratification phenomenon in I/S clays is accidental in each stage of the dissolution, precipitation, and growth, as mentioned above. Therefore, interstratified I/S clays as mineral species do not really exist during the conversion, but the well-known random I/S clays having 100–50% expandable layers can be regarded as smectite which is undergoing K-fixation and dissolution; the ordered I/S clays having 50–0% expandable layers can be regarded as immature or embryonic illite which is still growing.

In conclusion, according to the present hypothesis, all problems on the smectite-to-illite conversion can be ascribed to the kinetics of smectite dissolution and illite growth in natural environments. Furthermore, in terms of the phase problem of I/S clays (Garrels, 1984; Nadeau et al., 1984b; Wilson and Nadeau, 1985), randomly interstratified I/S clays can be considered as metastable, one-phase smectite solid solutions and ordered I/S clays can be also considered as metastable, one-phase illite solid solutions, arising from their finer particle size. On the other hand, a perfectly ordered rectorite mineral generally shows a different occurrence and mineralogic properties, compared to the familiar I/S clays (Inoue and Utada, 1983). True rectorite can be an interstratified mineral species and thereby should probably be excluded from the category of familiar I/S clays in question.

REFERENCES

Boles, J. R. and Franks, S. G. (1979) Clay diagenesis in Wilcox sandstones of southwest Texas: Implications of smectite diagenesis on sandstone cementation: J. Sed. Petrol. 49, 55–70.

Browne, P. R. L. and Ellis, A. J. (1970) The Ohaki-Broadlands hydrothermal area, New Zealand: Mineralogy and related geochemistry: Amer. J. Sci. 269, 97–131.

Cliff, G. and Lorimer, G. W. (1975) The quantitative analysis of thin specimens: J. Microsc. 103, 203–207.

Dunoyer de Segonzac, G. (1970) The transformation of clay minerals during diagenesis and low-grade metamorphism: A review: Sedimentology 15, 281–346.

Eslinger, E. V. and Savin, S. M. (1973) Mineralogy and oxygen isotope geochemistry of the hydrothermal altered rocks of the Ohaki-Broadlands, New Zealand geothermal area: Amer. J. Sci. 273, 240–267.

Foscolos, A. F. and Kodama, H. (1974) Diagenesis of clay minerals from lower Cretaceous shales of northeastern British Columbia: Clays & Clay Minerals 22, 319–336.

Garrels, R. M. (1984) Montmorillonite/illite stability diagrams: Clays & Clay Minerals 32, 161–166.

Güven, N. (1974) Lath-shaped units in fine-grained micas and smectites: Clays & Clay Minerals 22, 385–390.

Güven, N., Hower, W. F., and Davies, D. K. (1980) Nature of authigenic illites in sandstone reservoirs: J. Sed. Petrol. 50, 761–766.

Hoffman, J. and Hower, J. (1979) Clay mineral assemblages as low grade metamorphic geothermometers: Application to the thrust faulted Disturbed Belt of Montana, U.S.A.: Soc. Econ. Paleontol. Mineral. Spec. Publ. 26, 55–79.

Horton, D. G. (1985) Mixed-layer illite/smectite as a paleotemperature indicator in the Amethyst vein system, Creede district, Colorado, USA: Contrib. Miner. Petrol. 91, 171–179.

Hower, J. (1981) Shale diagenesis: in Clays and the Resource Geologist, F. J. Longstaffe, ed., Short Course Handbook 7, Mineral. Assoc. Canada, 60–80.

Hower, J., Eslinger, E., Hower, M., and Perry, E. (1976) The mechanism of burial diagenetic reactions in argillaceous sediments, 1. Mineralogical and chemical evidence: Geol. Soc. Amer. Bull. 87, 725–737.

Inoue, A., Minato, H., and Utada, M. (1978) Mineralogical properties and occurrence of illite/montmorillonite mixed layer minerals formed from Miocene volcanic glass in Waga-Omono district: Clay Sci. 5, 123–136.

Inoue, A. and Utada, M. (1983) Further investigations of a conversion series of dioctahedral mica/smectites in the Shinzan hydrothermal alteration area, northeast Japan: Clays & Clay Minerals 31, 401–412.

Jagodzinski, H. (1949) Eindimensionale Fehlordnung in Kristallen und ihr Einfluss auf die Röntgeninterferenzen. I.

Berechnung des Fehlordnungsgrades aus der Röntgenintensitaten: *Acta Crystallogr.* **2,** 201–207.

Jennings, S. and Thompson, G. R. (1986) Diagenesis in Plio-Pleistocene sediments in the Colorado River delta, southern California: *J. Sed. Petrol.* **56,** 89–98.

Muffler, L. J. P. and White, D. E. (1969) Active metamorphism of upper Cenozoic sediments in the Salton Sea geothermal fields and the Salton trough, southeastern California: *Geol. Soc. Amer. Bull.* **80,** 157–182.

Nadeau, P. H., Tait, J. M., McHardy, W. J., and Wilson, M. J. (1984a) Interstratified XRD characteristics of physical mixtures of elementary clay particles: *Clay Miner.* **19,** 67–76.

Nadeau, P. H., Wilson, M. J., McHardy, W. J., and Tait, J. M. (1984b) Interparticle diffraction: A new concept for interstratified clays: *Clay Miner.* **19,** 757–769.

Nadeau, P. H., Wilson, M. J., McHardy, W. J., and Tait, J. M. (1985) The conversion of smectite to illite during diagenesis: Evidence from some illitic clays from bentonites and sandstones: *Mineral. Mag.* **49,** 393–400.

Pollastro, R. M. (1985) Mineralogical and morphological evidence for the formation of illite at the expense of illite/smectite: *Clays & Clay Minerals* **33,** 265–274.

Reynolds, R. C. and Hower, J. (1970) The nature of interlayering in mixed-layer illite-montmorillonites: *Clays & Clay Minerals* **18,** 25–36.

Środoń, J. (1980) Precise identification of illite/smectite interstratifications by X-ray powder diffraction: *Clays & Clay Minerals* **28,** 401–411.

Środoń, J. and Eberl, D. D. (1984) Illite: in *Micas, Reviews in Mineralogy* **13,** S. W. Bailey, ed., Mineralogical Soc. Amer., 495–544.

Środoń, J., Morgan, D. J., Eslinger, E. V., Eberl, D. D., and Karlinger, M. R. (1986) Chemistry of illite/smectite and end-member illite: *Clays & Clay Minerals* **34,** 368–378.

Steiner, A. (1968) Clay minerals in hydrothermally altered rocks at Wairakei, New Zealand: *Clays & Clay Minerals* **16,** 193–213.

Watanabe, T. (1981) Identification of illite/montmorillonite interstratifications by X-ray powder diffraction: *J. Miner. Soc. Japan, Spec. Issue* **15,** 32–41 (in Japanese).

Weaver, C. E. and Beck, K. C. (1971) Clay water diagenesis during burial: How mud becomes gneiss: *Geol. Soc. Amer. Spec. Paper* **134,** 1–78.

Wilson, M. J. and Nadeau, P. H. (1985) Interstratified clay minerals and weathering process: in *The Chemistry of Weathering,* J. I. Drever, ed., NATO ASI series **C149,** Reidel, Dordrecht, 97–118.